Computer Methods and Programs in Biomedicine 219 (2022) 106751

Contents lists available at ScienceDirect

Computer Methods and Programs in Biomedicine

journal homepage: www.elsevier.com/locate/cmpb

Finite element analysis to predict short and medium-term performance of the anatomical Comprehensive® Total Shoulder System

Margarida Bola[a], José Simões[a,b], António Ramos[a,*]

[a] TEMA, Biomechanics Research Group, Department of Mechanical Engineering, University of Aveiro, Campo Universitário de Santiago, Aveiro 3810-193, Portugal

[b] ESAD- College of Art and Design, Avenida Calouste Gulbenkian, Senhora da Hora, Matosinhos 4460-268, Portugal

ARTICLE INFO

Article history:
Received 8 November 2021
Revised 8 March 2022
Accepted 10 March 2022

Keywords:
Pre-clinical test
Total shoulder arthroplasty
Finite element analysis
Clinical prediction

ABSTRACT

Background: The number of Total Shoulder Arthroplasties (TSA) has increased in these last years with significant increase of clinical success. However, glenoid component loosening remains the most common cause of failure.

Objective: In this study we evaluated the critical conditions to predict short and medium-term performance of the uncemented anatomical Comprehensive® Total Shoulder System using a finite element model that was validated experimentally.

Methods: The finite element models of an implanted shoulder analysed included total shoulder components with pegs. The models were simulated in 3 phases of adduction: 45°, 60° and 90° to determine the most critical situation. Two different bone-implant fixation conditions were considered: post-surgery and medium term (2 years).

Results: These show that the critical condition is for the shoulder in 90° adduction were the highest contact stress (70 MPa) was observed in the glenoid component. Relatively to the interface implant-bone strains, the maximum (-16000 $\mu\varepsilon$) was observed for the short-term in the lateral region of the humerus. The highest micromotions were observed in the central fixation post of the glenoid component, ranging from 20 to 25 µm, and 325 µm in the lateral plane of the humeral component.

Conclusion: The predicted results are in accordance with clinical studies published and micromotions of the humeral component can be used to predict loosening and to differentiate shoulder implant designs.

1. Introduction

Glenoid loosening is one of the major causes of failure in total shoulder arthroplasty (TSA) [1,2] and the incidence of early radiolucent glenoid lines has been reported to range from 22% to 95%. TSA as a standard of care uses all cemented glenoid components [3,4] with pegged implants performing better than keeled implants [5].

Several aspects are believed to be related with loosening of the glenoid component of the prosthesis [1], but failure of the implant-cement interface [6], fatigue failure and fragmentation of the poly (methyl methacrylate) (PMMA) cement layer [7] are some of the most significant. Some concerns regarding humeral stem fixation with cement have appeared and, because of this, uncemented humeral fixation has become more frequently used, but loosening and subsidence have been observed [8]. TSA clinical outcomes with hybrid glenoid components (Modular Hybrid® Glenoid Component) and with conventional cemented glenoid components (Bio-Modular® Shoulder System) were analysed during an average of 3.2 years at a minimum follow up of 2 years after surgery [9]. In this study, ten hybrid glenoid components were observed firmly fixed. The only complication registered in the hybrid component group was posterior instability, but new bone formed around the central post was observed. Jost et al. [10] analysed clinical outcomes of the Comprehensive® Humeral mini stem (Biomet®) and results evidence improved range-of-motion, abduction and internal and external rotation with no implant-related post-operative complications.

Schnetzke et al. [11] presented a radiographic analysis performed with 52 patients implanted with the uncemented short-stem humeral prosthesis (Aequalis Ascend Monolithic; Tornier, Grenoble, France) that can be considered in the same category of the Comprehensive Humeral Stem used in our study. The authors refer that radiologic evidences of bone adaptation are signs of stress shielding.

* Corresponding author.
E-mail address: a.ramos@ua.pt (A. Ramos).

https://doi.org/10.1016/j.cmpb.2022.106751
0169-2607/

Recently, Friedman et al. [12] reported a 50 months follow-up study were they compared hybrid and all-polyethylene peg cemented glenoid. The cage glenoid had significantly fewer radiolucent lines around both the glenoid and humeral components and a lower revision rate. A clinical review evidence some clinical important aspects and demonstrate that hybrid glenoid components provoke lower rates of radiolucent lines and failures in comparison to all-polyethylene glenoid [13].

Finite element models are largely used in or related biomechanics studies that allow to predict the behaviour of bone tissue in the vicinity of the implants. Several studies aimed the humeral components, but very few the anatomic glenoid component and total shoulder arthroplasty. Nikolas et al. [14] using a finite element model and considering only the scapular body, studied five different fixations in all-polyethylene glenoid components and conclude, relatively to micromovements, that the central pin and the model with 4 pegs are more stable. A recent study presents the effect of humeral thickness to study stresses in the humeral bone [15] suggesting that thinner implants with lower canal fill may be beneficial. Other models have been used to predict the behaviour of glenoid components in reverse shoulder arthroplasty by studying bone stresses and micromotions of pegs to predict implant stability [16]. The effect of pegs and glenoid perforation to predict implant stability and micromotions was study using finite element models [17].

The main objective of our study was to analyse the performance of a TSA with a hybrid glenoid connection to confirm the hypothesis that abduction at 90° is a critical position for the fixation of the glenoid component. Finite element analysis (FEA) were performed and stress and strains patterns correlated with load configurations simulated.

2. Materials and methods

2.1. Experimental and CAD model

The Comprehensive® TSA from Biomet® comprising the humeral and glenoid components was implanted in a composite intact shoulder model (scapula and humerus) from Sawbones manufacturer. These models allow to reconstruct the clinical position of the implants and are useful for experimental trials and to build reliable finite element models for simulations. The humeral component includes a porous (Regenerex® Porous Titanium) titanium stem in its superior part to provide biologic fixation. Fig. 1 shows all parts of the humeral component. The glenoid component has a curved back with an anatomic pear shape; the central peg is to provide fixation and is connected to the central hole of the base. The glenoid base is made of ultra-high molecular weight polyethylene (UHMWPE) with a metallic hole; the central peg is made of titanium with a Regenerex® layer.

Table 1
Material properties of bone structures used in simulations.

Structure	Young Modulus	Poisson ratio
Cortical humerus	16.5 GPa	0.3
Trabecular humerus	124 MPa	0.3
Cortical scapula	16 GPa	0.3
Trabecular scapula	E11 = 342 MPa E22 = 213 MPa E33 = 194 MPa G12 = G13 = G23 = 100 MPa	$\nu_{12} = \nu_{13} =$ $\nu_{23} = 0.26$
Titanium (humeral component and glenoid post)	110 GPa	0.3
Polyethylene (glenoid component)	1 GPa	0.4

The experimental TSA on a composite bone model was made by an expert surgeon (Fig. 1) following the press-fit technique as defined in the surgical protocol. The Computer Aided Design (CAD) models of the shoulder prosthesis were made to accurately replicate the experimental model. The position of the implant in the CAD model was obtained using 3D laser scanning (Roland Picza 3D) and the cortical layer was defined using CT scans of the bone geometry.

2.2. Finite element model

Software Abaqus CAE (V6.12©Dassault Systèmes) was used to perform the numerical simulations. A sensitive analysis for appropriate mesh size was previously performed and published elsewhere by the same authors of this paper [18]. The models are composed (506,568 degrees of freedom - DOF) of linear tetrahedral elements [19] of type C3D4 (4 nodes, 3 degrees of freedom per node) and are presented in Fig. 2. The mesh quality was controlled assuring an Average Aspect Ratio (AAR) less than 2 in all bodies and the percentage of elements with aspect ratio (AR) more than 3 remain below than 3%.

The mechanical properties of cortical and trabecular bone of the humerus and cortical bone of the scapular were modelled as isotropic linear elastic materials [20–22]. The scapular trabecular bone was modelled as an anisotropic linear elastic material [23,24] (Table 1) because that region of scapula presents the anisotropy of the glenoid cancellous bone properties [25]. Some authors refer

Fig. 1. Prosthesis components: humeral stem and humeral head, humeral adaptor and glenoid central post and glenoid base, in vitro models and CAD model.

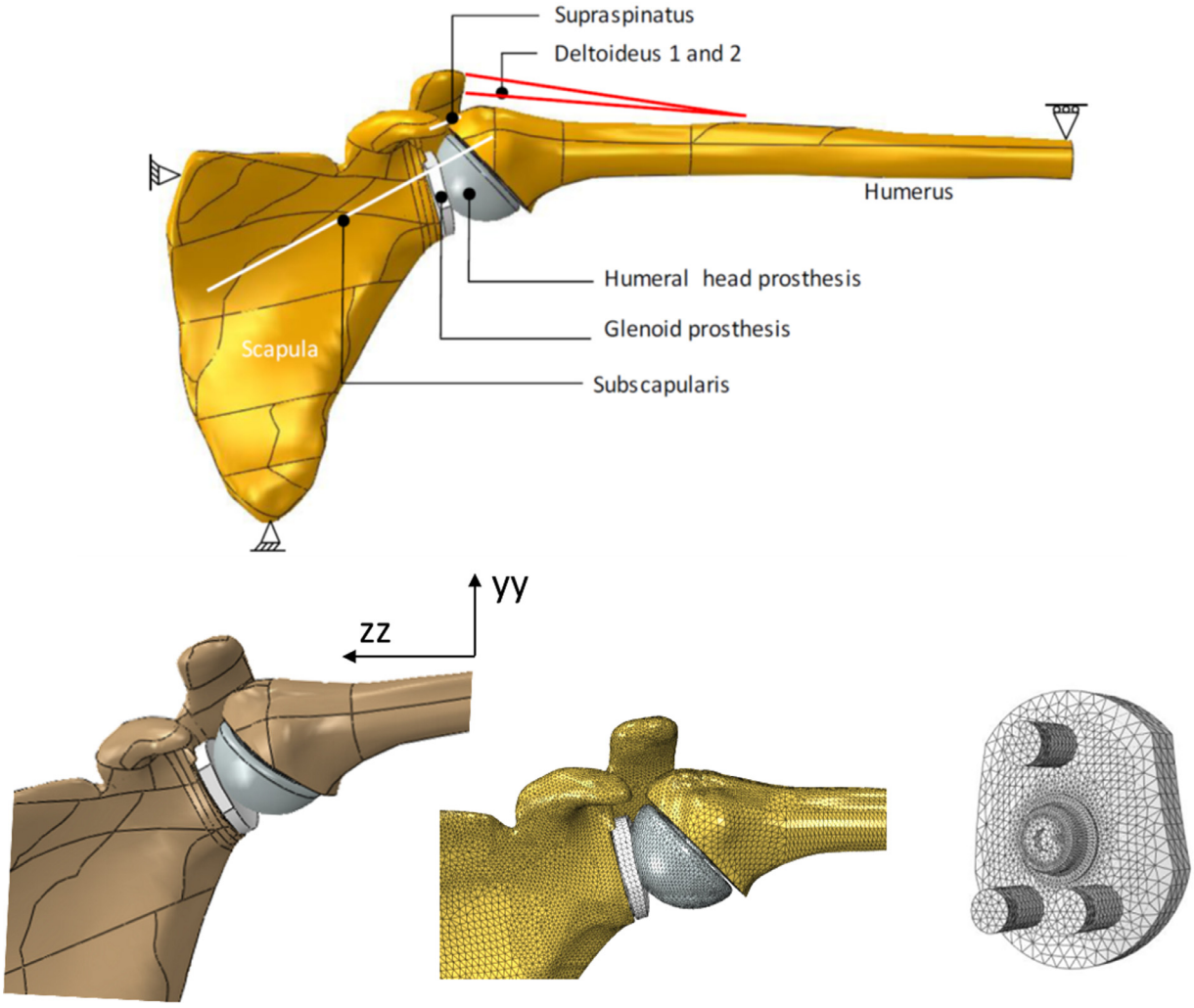

Fig. 2. CAD and finite element models of the implanted shoulder and muscular actions.

that this region is critical for implant behavior [26]. The muscular insertions considered are the same as those reported in a previous study [27]. The insertion in the bones was made using a large band fixed in the same area, similar to the same as other studies [28].

2.3. Boundary conditions

To understand the principles of uncemented shoulder prosthesis failure it is mandatory to define the most critical mechanical condition of the implant fixation. In this sense, the joint behaviour was compared in three abduction positions: 45°, 60° and 90°, and only considering the movement of the humerus (scapulothoracic rhythm was assumed). The models had the same muscle insertion sites and all prosthesis components were considered perfectly bonded to the surrounding bone. We considered the most important muscular actions defined in each abduction position (Table 2) and were determined using a multi-body model of the intact shoulder, considering 1 Kgf in hand and according to data measured in vivo by Bergmann et al. [29]. The scapular bone was supported in two points as presented in Fig. 2 and according to previous work [18], and could rotate in the lower support and a scapulohumeral rhythm of 5° was considered for 90° of abduction.

2.4. Interface conditions

Two post-operative scenarios were considered in the FEA to identify the most critical mechanical condition: short/medium-term and long-term. On the short/medium-term and post-operative condition simulated. The conditions do not represent the situation after surgery, because in a press-fit condition there are stress concentrations in the surrounded bone because the canal size is smaller than the stem size. After some days, bone adapts to the new biomechanical environment and stresses are released. For the short term condition a Coulomb friction condition at the in-

Table 2
Muscular actions.

Force (N)		Muscles				
		Deltoideus 1	Deltoideus 2	Subscapularis	Infraspinatus	Supraspinatus
Abduction Angle	45°	95	95	119	53	43
	60°	116	116	145	70	53
	90°	150	150	225	120	90

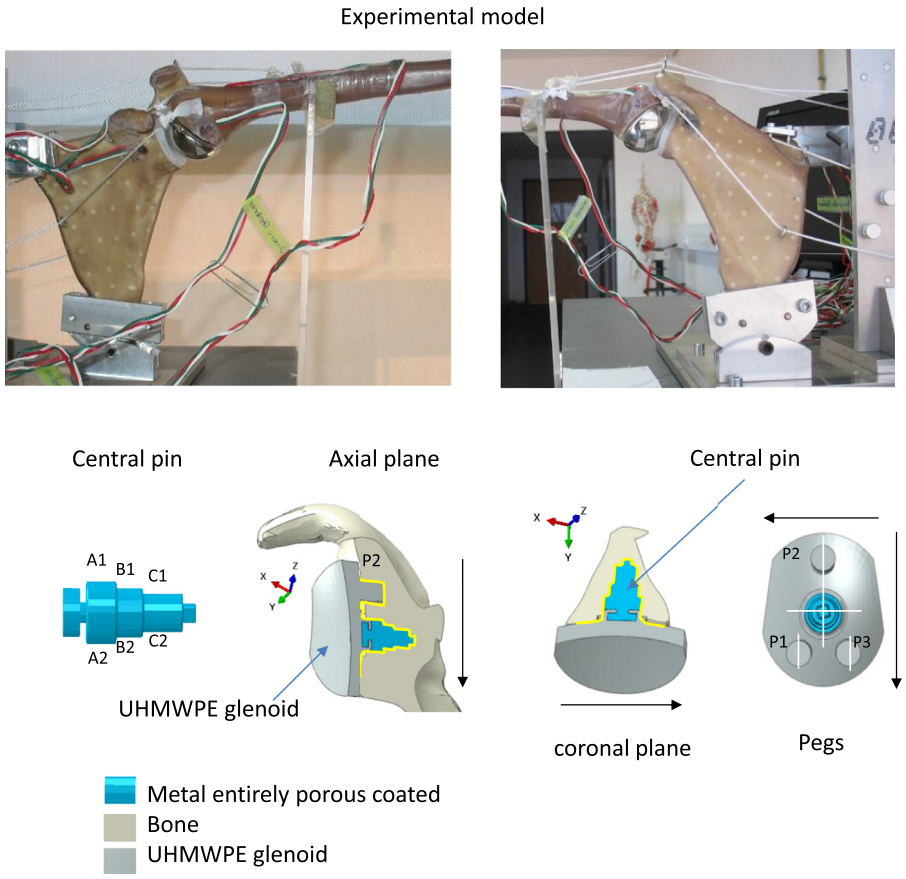

Fig. 3. Experimental procedure and definition of the regions on the glenoid component.

Table 3
Interface conditions (press-fit contact).

Surface pairs	Friction coefficient
Glenoid prosthesis/Glenoid bone	0.30
Glenoid central post/Glenoid trabecular bone	0.88
Porous surface of humeral component/Humeral bone	0.88
Smooth surface of humeral component/Humeral bone	0.40
Humeral head/ Glenoid prosthesis	0.1

terface was considered and is presented in Table 3. For the porous surface, a 0.88 friction coefficient was used [30] considering the contact node-to-surface. On the long-term post-operative scenario, the prosthesis was considered perfectly bonded to the surrounding bone as a surface-to-surface node tie. Results were analysed around the glenoid component.

According to Gulotta et al. [9], Fig. 3 shows the regions of the glenoid, the interfaces and position of the pegs for referencing. In the presence of friction, the humeral component (humerus and prosthesis) became unstable. To stabilize the model, a boundary condition at the base of the humeral shaft was considered and a symmetry constraint about the sagittal plane (X plane) was considered.

3. Results

The FE model was validated previously [31] through an experimental procedure (Fig. 3), obtaining a correlation value of 0.88 and a Root-Mean-Square-Error (RSME) of 69.7 με. The abduction angle influenced the location of the contact point between the two components of the prostheses. This point moved toward the centre of the glenoid prosthesis, increasing the abduction angles and staying in a posterior-superior region when in 90° abduction, with a maximum contact stress of 70 MPa.

3.1. Critical abduction position

To define the most critical condition, we analysed cortical and trabecular stress-strain distributions for the three abduction angles simulated (45°, 60°, 90°). We observed that the most critical biomechanical condition for the shoulder implant interface is during high abduction angles (90° in the present case). The principal stresses and strains were determined at the periphery of the superior and central holes of the glenoid bone (Fig. 3).

As illustrated in Fig. 4, compressive stresses and strains are more significant than tensile and are higher in the superior fixation hole (up and base periphery) at region A1, close to the central fixation post. It is clear that when the abduction angle augments, tensile and compressive stresses also augment and the same was observed for the humerus.

3.2. Clinical predictions and post-operative scenarios

The minimum principal strains for the intact condition on the short/medium-term and the predicted numerical glenoid principal compressive strains as shown in Fig. 5 considering the most critical situation (90° of abduction). The glenoid was divided in axial and coronal planes (Fig. 3) and regions of interest are identified as the same of those presented by Gulotta et al. [9]: 1 to 4 in the axial plane; and 5 to 8 in the coronal plane.

We observed that compressive strains are mainly in the range considered as physiological loading which, according to Roberts et al. [32], is from ≈ 200 to 2500 με. That range of strain indicates

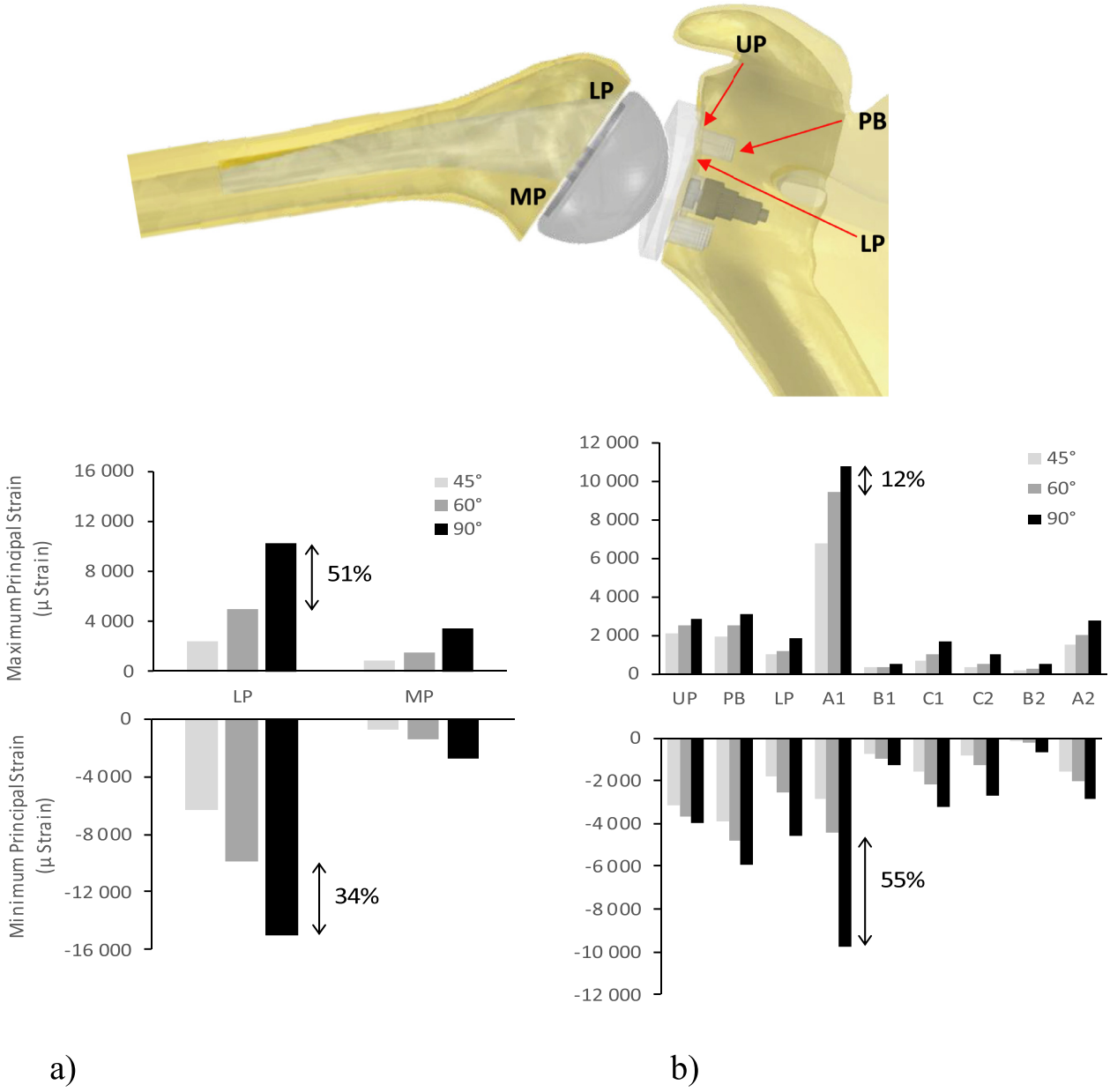

Fig. 4. Humerus and glenoid maximum tensile and compressive strains. a) Humerus strains; LP: lateral periphery; MP: medial periphery. b) Glenoid strains; UP: upper periphery; PB: peg base periphery; LP: lower periphery of the superior fixation hole; A1, A2, B1, B2, C1, C2: periphery of the central fixation post.

that the modular Hybrid® glenoid post used in this study seems to be an adequate clinical option for glenoid fixation, as bone density maintained within physiological values as well as bone integrity.

Close to the fixation holes we observed compressive strains in the range of 2500 to 4000 με, which means that these regions can be prone to bone hypertrophy with bone density augmentation. In some critical regions, strains are in the range of 4000 to 25,000 με, which means that trabecular bone is under very high compressive stresses and fracture can occur when strain repeatedly exceeds 4000 με (as in region 3), as well as prosthesis loosening.

The results considering the simulation of long-term condition show that compressive strains are mainly between 200 and 2500 με, in both axial and coronal planes. This indicates that for the long-term, the glenoid prosthesis is well fixed to the surrounding bone and bone integrity is maintained, despite the presence of the implant. On the axial plane, the compressive strains were between 2500 and 25,000 με on the short-term (see region 3 and 4) and in a smaller area on the long-term. This indicates that after the prosthesis is completely bonded to the surrounding bone there are regions with bone density augmentation (green area) and others were fatigue failure can occur (blue area).

In regions 1 and 2 (close to the central fixation hole), compressive strains are inferior than -200 με, which means that bone is not being sufficiently stimulated and bone resorption may occur. On the coronal plane, areas of fixation with high compressive strains were observed around the superior fixation peg and around the central fixation post, especially on the posterior and superior regions, similarly to what was observed for the short-term simulation condition. Compressive strains surpass 4000 με in some small areas around the fixation holes, which means that on the long-term there is still a possibility for bone fracture due to very high stresses observed. Low strains were observed between the polyethylene component and cortical bone. However, these strains

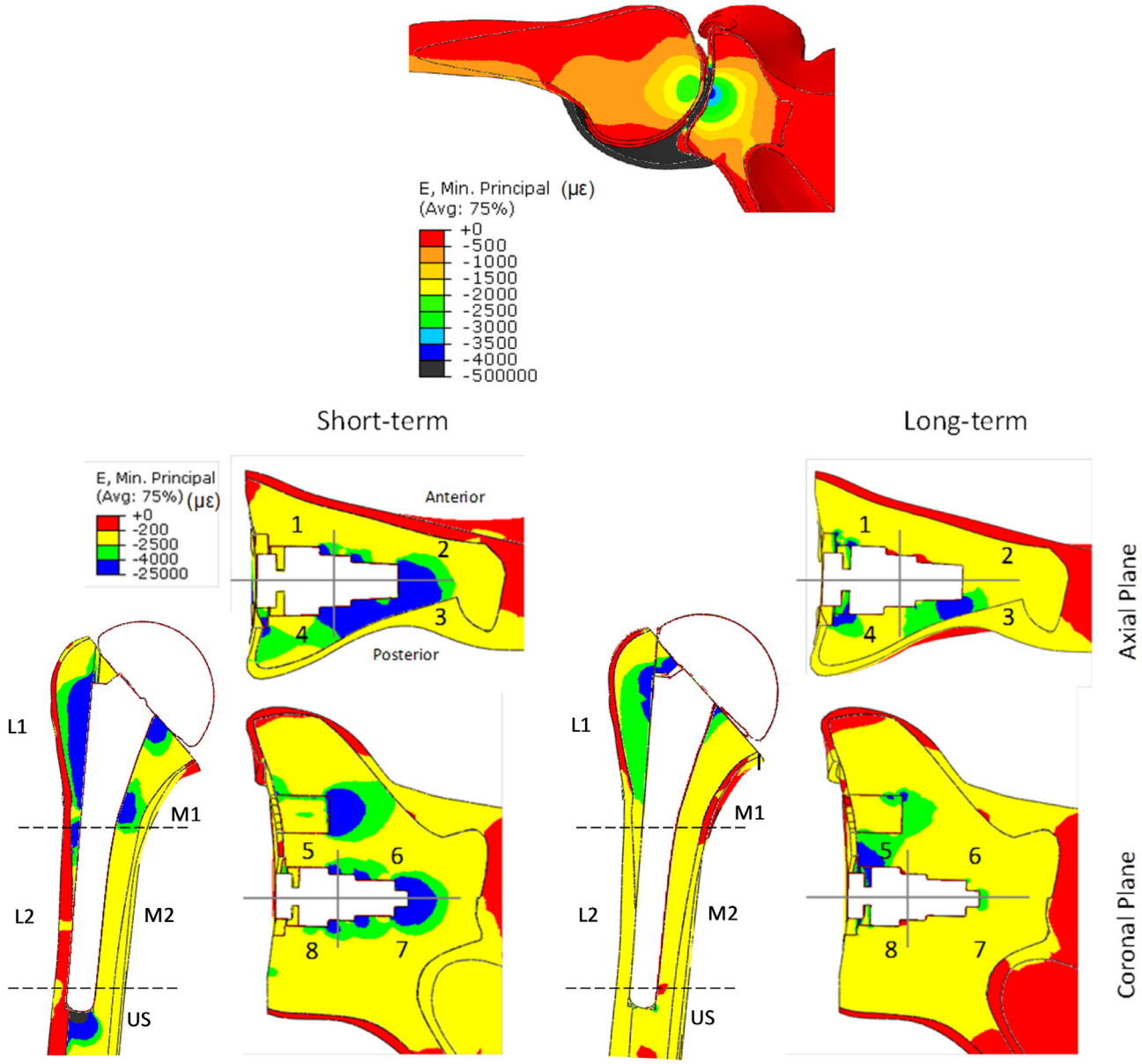

Fig. 5. Principal strains on intact shoulder for the implanted condition considering the short-term and long-term conditions according to Gulotta et al. [9].

are influenced by the implant position and may not represent the real situation.

Relatively to the humeral components, we divided them in medial (M1 and M2), lateral (L1 and L1) and under stem (US) regions, in accordance with Nagels et al. [33]. On the humerus trabecular bone, the majority of the compressive strains are in the range of physiologic ones. In region L1, bone is at risk since strain fractures due to fatigue failure close to the bone-implant interface can be as high as 25,000 $\mu\varepsilon$. The numerical simulations also show possible cortical thinning on the same region, since compressive strains, in the range of 0 to 200 $\mu\varepsilon$, are comparably low. The lack of the formation of new bone close to the implant may lead to loosening and to higher micromotions of the humeral component.

In region US, there are areas where trabecular bone is considered at risk by spontaneous fractures, since compressive strains exceed 25,000 $\mu\varepsilon$. There are also areas where principal strains promote bone hypertrophy by bone density augmentation. This may be related with the condensation lines around the tip that are considered as signs of stress shielding. In the tip we considered continuous support of cancel bone, which probably may not occur in most of the patients, but in a long term some clinical cases have shown bone formation, probably with different bone properties in the surrounding region of the tip of stem.

On the long-term analysis, most compressive strains are within the range of physiological bone loading, where bone integrity is maintained (200, 2500 $\mu\varepsilon$). In region L1 we observed areas of concern, since bone can suffer fatigue collapse. Nevertheless, bone remodelling with bone density increase can also be observed (green area). It is interesting to notice that on the short-term (region L1), the region where bone collapse may occur (blue area) is a region where bone remodelling may occur on the long-term (green area). This means that if bone has the capability to withstand strains on the short-term, there is a possibility that on the long-term it may become more resistance. In the lateral L2 region we observed contact between the stem and cortical bone due to the surgical approach.

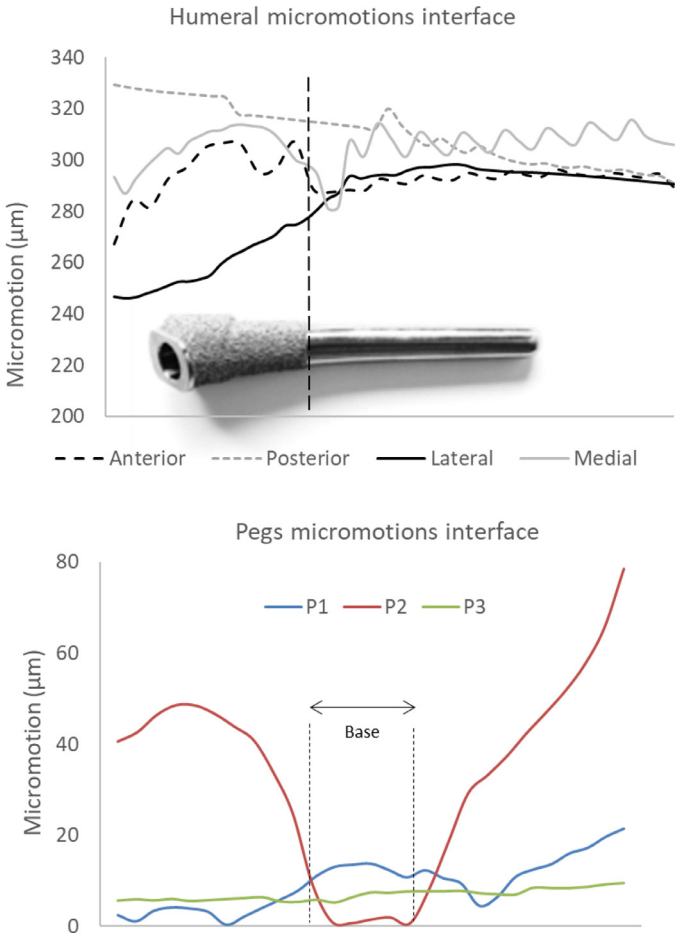

Fig. 6. Micromovements in the interface in the humeral and glenoid component in the pegs.

3.3. Bone interface micromotions

The highest micromotions observed on the central fixation post of the glenoid component are in the range of 20 to 25 μm, which can be considered optimum for bone ingrowth/ongrowth and are presented in Fig. 6. Micromotions are in the same range for the polyethylene fixation pegs. Additionally, higher micromotions observed on the top periphery peg ($>$ 20 μm) and smaller micromotions on the bottom ($<$ 15 μm) may indicate a tendency for the rocking horse phenomenon that is related to glenoid loosening. However, smaller micromotions of the central fixation post ($<$ 30 μm) indicate that the glenoid component is well fixed, which will avoid its loosening. The highest micromotions at the humeral component were observed posteriorly ($\approx$ 325 μm), whilst the smallest were observed laterally ($\approx$ 250 μm). These results are higher than 150 μm, and are an indication that prosthesis is prone to subsidence along the intramedullary canal, allowing the humerus to sink down the canal.

4. Discussion

In literature reviewed we observed that most studies do not include TSA, and some studies address the humeral or the glenoid component solely. For the conditions simulated in your study and inherent assumptions, the results show that the critical position for bone strain and implant stability is the abduction angle of 90°. Fixation of the hybrid glenoid component with a central porous titanium post evidenced good stability and fixation, which has been confirmed clinically [13].

The glenoid component has been the centre of discussion of prosthesis fixation in TSA [34–36], but the humeral implant has also raised doubts [37,38]. To try to overcome those, developments have been made in the humeral component fixation [39,40] and on the humeral stem design [41,42]. Within the analysis of the glenoid we observe that there is pronounced evidence of critical regions, mainly at the posterior-superior area of the cavity. Due to its high stiffness, the central post did not present any significant deformation, which may provoke strain-shielding that has been related clinically to loosening of the glenoid component. Regardless of this, our numerical results are in accordance with clinical outcomes [9], since strains at the glenoid cavity are within physiological loading ($\approx$ 200, 2500 $\mu\varepsilon$). Having said so, the modular Hybrid® glenoid post is an adequate option for uncemented glenoid fixation and will not obstruct the integrity of bone density inside the cavity that has been observed radiographically [8].

Gulotta et al. [9] presented clinical outcomes of the Comprehensive® Total Shoulder System (Biomet®) with a modular Hybrid® glenoid component. However, other clinical reports of modern glenoid non-cemented components [43–46] or minimally cemented [47–49] evidence low risk of glenoid loosening [9]. Most of these designs are made in polyethylene, with the central fixation post having flanges for bone integration and a central titanium core to provide necessary stiffness.

The radiolucent lines in the glenoid-cement interface are still frequently in pegs and keeled implants in the first years of implantation [12]. The radiolucent lines in the glenoid interface is a critical scenario for loosening according to the radiolucent line scoring method [50] and we observed grade 1 and 2 around pins in the long term similar to a clinical study performed after 50 months [12].

In addition, the relative micromotion between bone and implant is a major issue that must be considered regarding implant fixation. Leucht et al. (2008) compared bone formation in unloaded and loaded environments, with a dramatic increase when micromotion was present (150 μm). However, bone ingrowth does not always take place around porous-surfaced implants [9] and may not occur when micromotions are higher than 150 μm [16,51] as we observed in the humeral interface. Recently, Wahab et al. [24] determined maximum micromotions of 20.7 μm, 18.3 μm and 23.3 μm at bone-cement interface in centric, superior-anterior and superior-posterior loading conditions on a four pegged all-PE implant respectively. These results are similar to the ones presented, but comparisons must be performed critically and carefully, since simulation conditions may be different, namely those related with loading scenarios and due to the use of cement and all-PE glenoid component. The glenoid fixation component is a critical issue [14], and when the component is fully polyethylene, the Cross-Keel presents lower stability in comparison with the Central-Finned 4-Peg.

Suárez et al. [52] developed FEA studies and analyzed micromotion patterns of cementless glenoid components and the relationship with conforming designs and prosthesis positioning has been suggested [22]. However, the authors focused the study on a metal-backed implant with a central metallic fixation screw making any comparison with our model difficult to perform. The highest micromotions at the humeral component was observed posteriorly ($\approx$ 325 μm) while the smallest were observed laterally ($\approx$ 250 μm). According to literature [51], humeral stem micromotions are too high to allow bone ingrowth around its entire surface.

The experimental study with all-PE glenoid components having a centrally fluted peg (Anchor Peg Glenoid, DePuy Orthopaedics) and considering three different fixation methods was presented by Wiater et al. [53]. Interference-fit (also called press-fit), hybrid cement (cemented on the periphery pegs and uncemented on the central peg) and fully cemented were studied. Their results

suggest that the addition of cement on the peripheral pegs does not significantly improve initial fixation when compared with the interference-fit condition [12].

Other important aspect in the glenoid fixation and stabilization is the contact point of the shoulder arthroplasty. The anterior offsetting of glenoid has been associated with an increased contact area and a decreased peak pressure in the contact between the head and glenoid components, reducing instability which has been referred in other studies [54]. Shoulder becomes more stabilised when positioned more anteriorly. The FEA of the implanted shoulder developed in this study was made considering the stem inclination after observing that the humeral stem was introduced with some degree of tilting in the in vitro replacements made in our laboratory. It was interesting to note that there was a 5% incidence of humeral stem inclination on the shoulders analysed by Jost et al. [10], but this degree of inclination does not seem to affect the outcome clinical results.

Schnetzke et al. [11], based on a clinical study with the Aequalis Ascend Monolithic humeral component, claim that the results obtained through radiographs at 2 years after surgery, despite the presence of cortical thinning and density bone loss due to stress shielding (82.7% in the medial region, close to the humeral calcar). Their results are in accordance with our findings, since our simulations predicted cortical thinning and bone loss in similar areas as those observed clinically. However, the bulk humeral stem used [11] promotes load transfer mainly in regions L1 and M1, while the Comprehensive Humeral Stem presents higher stresses, mainly in region M1.

Relatively to the humeral coating, clinical studies have been performed to analyse proximally coated and uncoated short-stem humeral implants [55]. The mean follow-up study of 27.3 months revealed that uncoated stems seem to be at greater risk of loosening, in accordance with the study [49]. In our study, the humeral prosthesis used is coated on the proximal region and the high stresses and strains at the tip of the implant indicate subsidence, observed in only one shoulder (2.9% of a total of 34) in the clinical study. Normally in the tip region of stem we do not observe cancellous bone, and results should be addressed carefully. Strains in most of the proximal humerus are within the range considered as physiological, indicating that the proximally coated short-stem component is an option for uncemented humeral fixation, as it will not obstruct the integrity of bone density.

Micromotions of the humeral component are higher than 250 µm in all aspects (anterior, posterior, medial and lateral) and may be too high to allow bone ingrowth, but this effect was not observed clinically in proximally coated implants [10,11,56]. A possible explanation for these observations can be related with the friction coefficients considered in the simulation of the contact condition between the humeral stem and trabecular bone.

5. Study limitations

The use of composite bones is certainly a relevant limitation, but it is suitable for comparisons between different authors/groups studies, since it is a standard material/geometry structure. Another limitation of the FE model is related to the consideration of linear elastic behaviour and homogeneity of material of the bone structures. Another limitation of these type of studies is the impossibility to consider the effect of dynamic bone remodelling around implant, that can also play a significant role in the behaviour of the prosthesis.

6. Conclusions

The FEA developed simulates the behaviour of a TSA with an anatomical prosthesis integrating a porous coated central fixation post for glenoid fixation and with a porous-coated short-stem humeral component. The biomechanical critical condition within the implant-bone connection was observed when the joint is in the 90° abduction position.

Results obtained are in accordance with those observed clinically, especially for the glenoid component, and therefore it is possible to predict the performance of TSA for the short/medium-term and long-term using finite element models and respective analysis. A correlation was observed between the principal strains in the referred critical situation with clinical outcomes relatively to implant fixation. The predicted results are in accordance with clinical studies published and micromotions of the humeral component can be used to predict loosening and to differentiate shoulder implant designs.

Funding

This work was financially supported by the POCI-01-0145-FEDER-032486 project, funded by FEDER, through COMPETE2020 - Programa Operacional Competitividade e Internacionalização (POCI), and by national funds (OE), through FCT/MCTES.

Ethical statement

No ethical committees.

Declaration of Competing Interest

This author, their immediate family, and any research foundation with which they are affiliated did not receive any financial payments or other benefits from any commercial entity related to the subject of this article.

References

[1] A. Karelse, A. Van Tongel, T. Van Isacker, B. Berghs, L. De Wilde, Parameters influencing glenoid loosening, Expert Rev. Med. Dev. 13 (2016) 773–784, doi:10.1080/17434440.2016.1205483.
[2] G.C. Mallo, L. Burton, M. Coats-Thomas, S.D. Daniels, N.J. Sinz, J.J.P. Warner, Assessment of painful total shoulder arthroplasty using computed tomography arthrography, J. Shoulder Elb. Surg. 24 (2015) 1507–1511, doi:10.1016/j.jse.2015.06.027.
[3] G. Walch, P. Boileau, J.-F. Gonzalez, G.B. Alami, F. Baque, G. Walch, P. Boileau, Complications of unconstrained shoulder prostheses, J. Shoulder Elb. Surg. 20 (2011) 666–682, doi:10.1016/j.jse.2010.11.017.
[4] D.M. Kim, M. Aldeghaither, F. Alabdullatif, M.J. Shin, E. Kholinne, H. Kim, I.-H. Jeon, K.-H. Koh, Loosening and revision rates after total shoulder arthroplasty: a systematic review of cemented all-polyethylene glenoid and three modern designs of metal-backed glenoid, BMC Musculoskelet. Disord. 21 (2020) 114, doi:10.1186/s12891-020-3135-6.
[5] L.Fink Barnes, B.O. Parsons, E. Flatow, Pegged or keeled glenoid component use: which is it? Semin. Arthroplasty. 25 (2014) 246–249, doi:10.1053/j.sart.2015.02.007.
[6] J. Sarah, G. Sanjay, S. Sanjay, A. Carolyn, R. Emery, A. Andrew, H. Ulrich, Failure mechanism of the all-polyethylene glenoid implant, J. Biomech. 43 (2010) 714–719, doi:10.1016/j.jbiomech.2009.10.019.
[7] R. Vaishya, M. Chauhan, A. Vaish, Bone cement, J. Clin. Orthop. Trauma. 4 (2013) 157–163, doi:10.1016/j.jcot.2013.11.005.
[8] C.G. Nelson, T.J. Brolin, M.C. Ford, R.A. Smith, F.M. Azar, T.W. Throckmorton, Five-year minimum clinical and radiographic outcomes of total shoulder arthroplasty using a hybrid glenoid component with a central porous titanium post, J. Shoulder Elb. Surg. 27 (2018) 1462–1467, doi:10.1016/j.jse.2018.01.012.
[9] L.V. Gulotta, K.L. Chambers, R.F. Warren, D.M. Dines, E.V. Craig, No differences in early results of a hybrid glenoid compared with a pegged implant, Clin. Orthop. Relat. Res. 473 (2015) 3918–3924, doi:10.1007/s11999-015-4558-5.
[10] P.W. Jost, J.S. Dines, M.H. Griffith, M. Angel, D.W. Altchek, D.M. Dines, Total shoulder arthroplasty utilizing mini-stem humeral components: technique and short-term results, HSS J 7 (2011) 213–217, doi:10.1007/s11420-011-9221-4.
[11] M. Schnetzke, S. Coda, P. Raiss, G. Walch, M. Loew, Radiologic bone adaptations on a cementless short-stem shoulder prosthesis, J. Shoulder Elb. Surg. 25 (2016) 650–657, doi:10.1016/j.jse.2015.08.044.
[12] R.J. Friedman, E. Cheung, S.G. Grey, P.H. Flurin, T.W. Wright, J.D. Zuckerman, C.P. Roche, Clinical and radiographic comparison of a hybrid cage glenoid to a cemented polyethylene glenoid in anatomic total shoulder arthroplasty, J. Shoulder Elb. Surg. 28 (2019) 2308–2316, doi:10.1016/j.jse.2019.04.049.

[13] E.M. Marigi, T.R. Duquin, T.Q. Throckmorton, J.W. Sperling, Hybrid fixation in anatomic shoulder arthroplasty: surgical technique and review of the literature, JSES Rev. Reports, Tech. 1 (2021) 113–117, doi:10.1016/J.XRRT.2021.01.005.
[14] N.K. Knowles, G.D.G. Langohr, G.S. Athwal, L.M. Ferreira, Polyethylene glenoid component fixation geometry influences stability in total shoulder arthroplasty, Comput. Methods Biomech. Biomed. Engin. 22 (2019) 271–279, doi:10.1080/10255842.2018.1551526.
[15] S. Synnott, G.D.G. Langohr, J.M. Reeves, J.A. Johnson, G.S. Athwal, The effect of humeral implant thickness and canal fill on interface contact and bone stresses in the proximal humerus, JSES Int 5 (2021) 881–888, doi:10.1016/J.JSEINT.2021.05.006.
[16] N. Bonnevialle, L. Geais, J.H. Müller, J. Berhouet, Effect of RSA glenoid baseplate central fixation on micromotion and bone stress, JSES Int 4 (2020) 979–986, doi:10.1016/J.JSEINT.2020.07.004.
[17] A.H.A. Wahab, A.P.M. Saad, A. Syahrom, M.R.A. Kadir, In silico study of glenoid perforation during total shoulder arthroplasty: the effects on stress & micromotion, Comput. Methods Biomech. Biomed. Engin. 23 (2020) 182–190, doi:10.1080/10255842.2019.1709828.
[18] A.M. Bola, A. Ramos, J.A. Simões, Sensitivity analysis for finite element modeling of humeral bone and cartilage, Biomater. Biomech. Bioeng. 3 (2016) 71–84.
[19] A. Ramos, J.A. Simoes, Tetrahedral versus hexahedral finite elements in numerical modelling of the proximal femur, Med. Eng. Phys. 28 (2006) 916–924, doi:10.1106/j.medengphy.2005.12.006.
[20] L. Peng, J. Bai, X. Zeng, Y. Zhou, Comparison of isotropic and orthotropic material property assignments on femoral finite element models under two loading conditions, Med. Eng. Phys. 28 (2006) 227–233, doi:10.1016/j.medengphy.2005.06.003.
[21] S. Gupta, F.C.T. van der Helm, F. van Keulen, F.C.T. Van Der Helm, F. Van Keulen, Stress analyses of cemented glenoid prosthesis in total shoulder arthroplasty, J. Biomech. 37 (2004) 1777–1786, doi:10.1016/j.jbiomech.2004.02.001.
[22] D.R. Suárez, J.C. van der Linden, E.R. Valstar, P. Broomans, G. Poort, P.M. Rozing, F. van Keulen, Influence of the positioning of a cementless glenoid prosthesis on its interface micromotions, Proc. Inst. Mech. Eng. H. 223 (2009) 795–804, doi:10.1243/09544119JEIM545.
[23] B. Couteau, P. Mansat, E. Estivalèzes, R. Darmana, M. Mansat, J. Egan, Finite element analysis of the mechanical behavior of a scapula implanted with a glenoid prosthesis, Clin. Biomech. (Bristol, Avon) 16 (2001) 566–575.
[24] A. Hadi, A. Wahab, M. Rafiq, A. Kadir, M. Noor, H. Tunku, K. Ardiyansyah, Number of pegs influence focal stress distributions and micromotion in glenoid implants : a finite element study, Med. Biol. Eng. Comput. (2016), doi:10.1007/s11517-016-1525-6.
[25] I. Kalouche, J. Crépin, S. Abdelmoumen, D. Mitton, G. Guillot, O. Gagey, Mechanical properties of glenoid cancellous bone, Clin. Biomech. 25 (2010) 292–298, doi:10.1016/J.CLINBIOMECH.2009.12.009.
[26] A. Terrier, R. Obrist, F. Becce, A. Farron, Cement stress predictions after anatomic total shoulder arthroplasty are correlated with preoperative glenoid bone quality, J. Shoulder Elb. Surg. 26 (2017) 1644–1652, doi:10.1016/J.JSE.2017.02.023.
[27] M. Bola, J. Simões, A. Ramos, Finite element model validation based on an experimental model of the intact shoulder joint, Med. Eng. Phys. 87 (2021) 1–8, doi:10.1016/j.medengphy.2020.11.004.
[28] A.E. Kedgley, G.A. Mackenzie, L.M. Ferreira, D.S. Drosdowech, G.J.W. King, K.J. Faber, J.A. Johnson, The effect of muscle loading on the kinematics of in vitro glenohumeral abduction, J. Biomech. 40 (2007) 2953–2960, doi:10.1016/j.jbiomech.2007.02.008.
[29] G. Bergmann, F. Graichen, A. Bender, A. Rohlmann, A. Halder, A. Beier, P. Westerhoff, In vivo gleno-humeral joint loads during forward flexion and abduction, J. Biomech. 44 (2011) 1543–1552, doi:10.1016/j.jbiomech.2011.02.142.
[30] Y. Zhang, P.B. Ahn, D.C. Fitzpatrick, A.D. Heiner, R.A. Poggie, T.D. Brown, Interfacial frictional behavior: cancellous bone, cortical bone, and a novel porous tantalum biomaterial, J. Musculoskelet. Res. 03 (1999) 245–251, doi:10.1142/S0218957799000269.
[31] M. Bola, J.A. Simões, A. Ramos, Finite element modelling and experimental validation of a total implanted shoulder joint, Comput. Methods Progr. Biomed. 207 (2021) 106158, doi:10.1016/J.CMPB.2021.106158.
[32] W.E. Roberts, S. Huja, J.A. Roberts, Bone modeling: biomechanics, molecular mechanisms, and clinical perspectives, Semin. Orthod. 10 (2004) 123–161, doi:10.1053/j.sodo.2004.01.003.
[33] J. Nagels, M. Stokdijk, P.M. Rozing, Stress shielding and bone resorption in shoulder arthroplasty, J. Shoulder Elb. Surg. 12 (2003) 35–39, doi:10.1067/mse.2003.22.
[34] M. Schrumpf, T. Maak, S. Hammoud, E.V. Craig, The glenoid in total shoulder arthroplasty, Curr. Rev. Musculoskelet. Med. 4 (2011) 191–199, doi:10.1007/s12178-011-9096-5.
[35] S. Urgery, I. Ncorporated, A. Papadonikolakis, N. Mb, M. Fa, Failure of the glenoid component in anatomic total shoulder arthroplasty, J. Bone Jt. Surg. 95-A (2013) 2205–2212, doi:10.2106/JBJS.L.00552.
[36] N. Bonnevialle, B. Melis, L. Neyton, L. Favard, D. Molé, G. Walch, P. Boileau, Aseptic glenoid loosening or failure in total shoulder arthroplasty: revision with glenoid re-implantation, J. Shoulder Elb. Surg. 22 (2013) 745–751, doi:10.1016/j.jse.2012.08.009.
[37] T.E. Harris, C.M. Jobe, Q.G. Dai, Fixation of proximal humeral prostheses and rotational micromotion, J. Shoulder Elb. Surg. 9 (2000) 205–210, doi:10.1067/mse.2000.105625.
[38] J. Sanchez-sotelo, T.W. Wright, S.W.O. Driscoll, R.H. Cofield, C.M. Rowland, Radiographic assessment of uncemented humeral components in total shoulder arthroplasty, 16 (2001) 180–187. doi:10.1054/arth.2001.20905.
[39] R.B. Litchfield, M.D. McKee, R. Balyk, S. Mandel, R. Holtby, R. Hollinshead, D. Drosdowech, S.E. Wambolt, S.H. Griffin, R. McCormack, Cemented versus uncemented fixation of humeral components in total shoulder arthroplasty for osteoarthritis of the shoulder: a prospective, randomized, double-blind clinical trial-A JOINTs Canada Project, J. Shoulder Elb. Surg. 20 (2011) 529–536, doi:10.1016/j.jse.2011.01.041.
[40] W.H. Seitz, Humeral component fixation, Semin. Arthroplasty. 19 (2008) 64–73, doi:10.1053/j.sart.2007.12.026.
[41] L. Harmer, T. Throckmorton, J.W. Sperling, Total shoulder arthroplasty: are the humeral components getting shorter? Curr. Rev. Musculoskelet. Med. 9 (2016) 17–22, doi:10.1007/s12178-016-9313-3.
[42] R.S. Churchill, G.S. Athwal, Stemless shoulder arthroplasty—current results and designs, Curr. Rev. Musculoskelet. Med. 9 (2016) 10–16, doi:10.1007/s12178-016-9320-4.
[43] L. De Wilde, N. Dayerizadeh, F. De Neve, C. Basamania, A. Van Tongel, Fully uncemented glenoid component in total shoulder arthroplasty, J. Shoulder Elb. Surg. 22 (2013) 1–7, doi:10.1016/j.jse.2013.01.036.
[44] G. Merolla, G. Merolla, Total shoulder arthroplasty with a second- generation tantalum trabecular metal-backed glenoid component: Clinical and radiographic outcomes at a mean follow-up of 38 months, Bone Jt. J. 98-B (2016), doi:10.1302/0301-620X.98B1.36620.
[45] M.D. Budge, E.M. Nolan, M.H. Heisey, K. Baker, J.M. Wiater, Results of total shoulder arthroplasty with a monoblock porous tantalum glenoid component: a prospective minimum 2-year follow-up study, J. Shoulder Elb. Surg. 22 (2013) 535–541, doi:10.1016/j.jse.2012.06.001.
[46] W.H.S. Jr, P. Marinello, J. Styron, The cemented humerus and non-cemented glenoid: The optimal hybrid solution for total shoulder arthroplasty, Semin. Arthroplasty. 27 (2016) 98–103, doi:10.1053/j.sart.2016.08.002.
[47] G.I. Groh, Survival and radiographic analysis of a glenoid component with a cementless fluted central peg, J. Shoulder Elb. Surg. 19 (2010) 1265–1268, doi:10.1016/j.jse.2010.03.012.
[48] A. Vidil, P. Valenti, F. Guichoux, J.H. Barthas, CT scan evaluation of glenoid component fixation: a prospective study of 27 minimally cemented shoulder arthroplasties, Eur. J. Orthop. Surg. Traumatol. 23 (2013) 521–525, doi:10.1007/s00590-012-1126-5.
[49] D.L. Parks, D.J. Casagrande, M.A. Schrumpf, S.M. Harmsen, T.R. Norris, J.D.K. Ii, Radiographic and clinical outcomes of total shoulder arthroplasty with an all-polyethylene pegged bone ingrowth glenoid component: prospective short- to medium-term follow-up, J. Shoulder Elb. Surg. 25 (2016) 246–255, doi:10.1016/j.jse.2015.07.008.
[50] M.D. Lazarus, K.L. Jensen, C. Southworth, F.A. Matsen, The radiographic evaluation of keeled and pegged glenoid component insertion, J. Bone Jt. Surg. - Ser. A. (2002), doi:10.2106/00004623-200207000-00013.
[51] S. Goodman, P. Aspenberg, Effect of amplitude of micromotion on bone ingrowth into titanium chambers implanted in the rabbit tibia, Biomaterials 13 (1992) 944–948, doi:10.1016/0142-9612(92)90118-8.
[52] W.Nerkens Suárez, E.R. Valstar, P.M. Rozing, F. Van Keulen, Interface micromotions increase with less-conforming cementless glenoid components, J. Shoulder Elb. 21 (2012) 474–482, doi:10.1016/j.jse.2011.03.008.
[53] J.E. Moravek, M.D. Kurdziel, K.C. Baker, J.M. Wiater, Biomechanical evaluation of all-polyethylene pegged bony ingrowth glenoid fixation techniques on implant micromotion, Am. J. Orthop. (2016) E211–E216.
[54] G.S. Lewis, W.K. Conaway, H. Wee, H.M. Kim, Effects of anterior offsetting of humeral head component in posteriorly unstable total shoulder arthroplasty: Finite element modeling of cadaver specimens, J. Biomech. (2017), doi:10.1016/j.jbiomech.2017.01.010.
[55] M.P. Morwood, P.S. Johnston, G.E. Garrigues, Proximal ingrowth coating decreases risk of loosening following uncemented shoulder arthroplasty using mini-stem humeral components and lesser tuberosity osteotomy, J. Shoulder Elb. Surg. 26 (2017) 1246–1252, doi:10.1016/j.jse.2016.11.041.
[56] M. Schnetzke, S. Coda, G. Walch, M. Loew, Clinical and radiological results of a cementless short stem shoulder prosthesis at minimum follow-up of two years, Int. Orthop. 39 (2015) 1351–1357, doi:10.1007/s00264-015-2770-2.